

See discussions, stats, and author profiles for this publication at: <https://www.researchgate.net/publication/229897744>

Surface segregation in conformationally asymmetric polymer blends: Incompressibility and boundary conditions

ARTICLE *in* THE JOURNAL OF CHEMICAL PHYSICS · APRIL 1996

Impact Factor: 2.95 · DOI: 10.1063/1.471272

CITATIONS

34

READS

8

3 AUTHORS, INCLUDING:



David Wu

Colorado School of Mines

98 PUBLICATIONS 1,667 CITATIONS

SEE PROFILE



Glenn H Fredrickson

University of California, Santa Barbara

434 PUBLICATIONS 28,398 CITATIONS

SEE PROFILE

Surface segregation in conformationally asymmetric polymer blends: Incompressibility and boundary conditions

David T. Wu and Glenn H. Fredrickson

Department of Chemical Engineering, University of California, Santa Barbara, California 93106

Jean-Pierre Carton

Service de Physique de l'Etat Condensé, CEA-Saclay, F-91191 Gif-sur-Yvette Cedex, France

(Received 15 December 1995; accepted 8 January 1996)

Recent experiments, analytical theory, and simulations have raised and examined the possibility of entropically driven segregation effects in conformationally asymmetric polymer blends. We consider herein a model of surface segregation in a molten blend of two polymers with different flexibilities as characterized by the pure-component parameter $\beta^2 = R_g^2/V_{\text{mol}}$, where R_g is the radius of gyration and V_{mol} is the molecular volume of a polymer chain. Analytic solutions to the self-consistent field equations are presented for small deviations of the conformational asymmetry parameter $\epsilon = (\beta_A/\beta_B)^2$ from unity. Even in the absence of enthalpic interactions with the wall, we find an effective exchange surface potential of entropic origin, which can be understood in terms of an imperfect screening of the wall by the self-consistent potential. We find that the more flexible component segregates to the surface, in qualitative agreement with an earlier density functional calculation, but with a different parameterization of the surface potential. For weak conformational asymmetry, the magnitude of the segregation is found to be proportional to $(\epsilon - 1)$, and inversely proportional to the bulk screening length of the total monomer density. Our analysis indicates that unlike single-component melts, where reflecting boundary conditions are appropriate, molten blends near a surface are described by an effective mixed boundary condition on the polymer Green's function $G(z, z'; s, s')$ of the form $\partial_z G \propto UG$, where U is the strength of the surface potential. In the perturbative limit, $|\epsilon - 1| \ll 1$, this proves equivalent to effective constant flux boundary conditions.

© 1996 American Institute of Physics. [S0021-9606(96)51414-9]

I. INTRODUCTION

Many applications of polymer materials rely on their interfacial or surface properties, which can differ significantly from corresponding properties in the bulk. This is particularly the case in multicomponent systems, such as blends or copolymers, where one species is often favored at the surface for enthalpic or entropic reasons.¹ Evidently, a fundamental theoretical understanding of the chemical and physical principles that control surface segregation in such systems could be extremely useful in tailoring surface properties.

Recent experiments probing surface enrichment in blends and block copolymers composed of polyolefin materials with a variety of microstructures^{2,3} have stimulated considerable interest in the surface properties of this important class of materials. Experiments on binary systems by the Bates' group³ suggest that the "sign" of the surface enrichment (i.e., which of the two components is favored at the surface) can be qualitatively understood by comparing the statistical segment lengths of the two species, provided segments are defined to occupy equal volumes. This enrichment principle can be most easily stated by defining the following pure component parameters for species $K=A$ or B :

$$\beta_K^2 = b_K^2 / (6v_K),$$

where b_K is the statistical segment length and v_K is the segment volume for type- K segments. The principle established by the Bates' group (based on measurements for a number of

olefin microstructures on a variety of surfaces) is that the component with the *smaller* value of β_K is enriched at the surface. Thus for a binary polymer blend with $\beta_B < \beta_A$, species B would be found in excess of its bulk concentration near the surface.

One interpretation of this "smallest β principle" is that the chains with smaller values of β are *entropically* favored at the surface of a polymer melt. Fredrickson and Donley⁴ presented a density functional theory to argue that this is indeed the case, although as will be discussed below, their theory suffers from quantitative defects. Another interpretation, gleaned from simulations carried out by Yethiraj,⁵ is that chains with the weakest cohesive forces are preferred at the surface in order to minimize the overall interaction energy. However, recent experiments by the Exxon/Princeton group⁶ have established a strong linear correlation between the value of β_K and the solubility parameter, δ_K , for a number of polyolefins. Thus polyolefins with the smallest β 's also have the weakest cohesive forces and are *enthalpically* favored at a low energy surface.

A simple scaling theory can be constructed to illustrate the interplay of these entropic and enthalpic factors. For this purpose, we imagine a blend of type A and B homopolymers at an interface with a poor, neutral solvent. (The presence of the solvent helps in developing scaling relations, but otherwise plays a minimal role. Thus we expect similar results regardless of whether the other phase is a solvent, a solid

substrate, vacuum, or air.) In situations where the segregation between components is weak, a simple approximation for the interfacial energy per unit area is $F_s \sim \gamma_A \phi_1 + \gamma_B(1 - \phi_1)$, where γ_K denotes the pure-component surface tension of species K and ϕ_1 is the volume fraction of species A in the layer of polymer very near the surface. Discarding the constant term, this can be written $F_s \sim \mu_1 \phi_1$, where $\mu_1 \sim \gamma_A - \gamma_B$ is a surface exchange chemical potential field. Next, we formulate a scaling estimate for μ_1 . For a melt of pure species K at the interface, the Helfand–Tagami theory⁷ suggests an interfacial width of order $\xi_K \sim \beta_K / \sqrt{\alpha_K}$. Here, α_K is the interaction density of species K with the poor solvent ($\alpha_K v_K$ is a Flory chi parameter between polymer K and solvent). The interfacial tension is correspondingly (energy units of $k_B T$) $\gamma_K \sim \alpha_K \xi_K \sim \beta_K \sqrt{\alpha_K}$. Thus we arrive at an exchange surface potential of the form

$$\mu_1 \sim \beta_A \sqrt{\alpha_A} - \beta_B \sqrt{\alpha_B}. \quad (1.1)$$

From this equation, we obtain a “modified β principle:” The species with the smallest value of $\beta_K \sqrt{\alpha_K}$ is enriched at the surface.

If the two polymers have similar cohesive forces and interactions with the solvent, then $\alpha_A \approx \alpha_B \approx \alpha$ and we obtain

$$\mu_1 \sim \sqrt{\alpha}(\beta_A - \beta_B) \sim \frac{\beta_K}{\xi_K}(\beta_A - \beta_B). \quad (1.2)$$

In this situation, *entropy* dominates and the surface is enriched by the more flexible (smaller β_K) species. This limit recovers the qualitative findings of Fredrickson and Donley,⁴ although they failed to predict the dependence on the interfacial width ξ_K .

In contrast, if the two polymers have comparable β_K 's, but different cohesive forces, then the Yethiraj arguments are recovered. This is particularly evident if we use regular solution theory⁸ to relate the interaction densities to the solubility parameters of the polymers, δ_K , and solvent, δ_S , i.e., $\alpha_K \sim (\delta_K - \delta_S)^2$. Then, at a low energy surface (e.g., air) we can neglect δ_S in comparison with δ_K , and one obtains

$$\mu_1 \sim \beta_A \delta_A - \beta_B \delta_B. \quad (1.3)$$

For comparable β_K 's, the species with the smaller δ_K (i.e., cohesive energy density) is favored at the surface for *enthalpic* reasons. As previously mentioned, for certain classes of polyolefins it appears that δ_K is proportional to β_K ,⁶ so in such systems the species with the smaller value of $\beta_K \delta_K$ is likely favored at the surface for *both* enthalpic and entropic reasons. While local packing effects associated with the detailed shapes of the monomers^{5,9} (not included in the above scaling picture) might also contribute to surface enrichment in polyolefins, we are not aware of any convincing experimental evidence of this to date.

In the present paper, we reexamine the case of segregation for *purely entropic* reasons and attempt a first-principles derivation of the scaling result summarized in Eq. (1.2). Using self-consistent field theory, we not only confirm that scaling relation, but explicitly derive an expression for the constant prefactor. Moreover, our analysis clarifies the fail-

ure of the Fredrickson–Donley density functional approach to recover Eq. (1.2) and provides some very useful results regarding the appropriate boundary conditions to be imposed on the field-theoretic propagators (Green's functions) for multicomponent polymer melts at surfaces. A systematic analysis of such boundary conditions has not hitherto been presented in the literature.

For a one-component melt against a repulsive surface (wall), we confirm that reflecting boundary conditions are appropriate for the single-chain propagators, giving rise in the case of near incompressibility to a flat profile up to a microscopic length from the wall. While in a blend this same profile is expected for the total density, the composition profile is nonuniform over a longer length scale and requires nontrivial *constant flux* boundary conditions. The subtlety in treating the effect of the surface lies in describing within a unifying framework how strictly absorbing boundary conditions (appropriate for hard walls¹⁰), when microscopic length scales are treated explicitly, give rise to effective boundary conditions for the “outer” or slowly decaying portion of the composition profile. A crude (but sufficient) treatment of the microscopic scales is available within the familiar self-consistent mean-field theory of polymer solutions.¹⁰ In the present paper, we adopt this approach, treating a polymer melt as a concentrated solution, and ultimately taking the limit of small solvent content (near incompressibility).

II. SELF-CONSISTENT FIELD THEORY

We consider a blend of two polymer species, which we label A and B . Each polymer of species K (where $K=A$ or B) consists of N_K statistical segments having volume v_m and length b_K . For convenience and without loss of generality, we have chosen to define the monomers of both polymers to be of equal volume. Having done so, however, the statistical segment lengths are in general different. This difference, or “conformational asymmetry,” can be parametrized by the ratio

$$\epsilon = \left(\frac{\beta_A}{\beta_B} \right)^2, \quad (2.1)$$

where β_K is the combination of pure component parameters encountered previously

$$\beta_K^2 \equiv \frac{R_{g,K}^2}{V_{\text{mol},K}} = \frac{b_K^2}{6v_m} \quad (2.2)$$

and is illustrated in Fig. 1. Since both the molecular volume, $V_{\text{mol},K} = N_K v_m$, and the square of the radius of gyration, $R_{g,K}^2 \equiv N_K b_K^2 / 6$, scale linearly with N_K in the melt, the parameter β_K is independent of chain length and definition of monomer. Rather, it is a local quantity that is a measure of “stiffness,” in the sense of distance spanned on the same chain per volume of polymer. (Note that this quantity we call

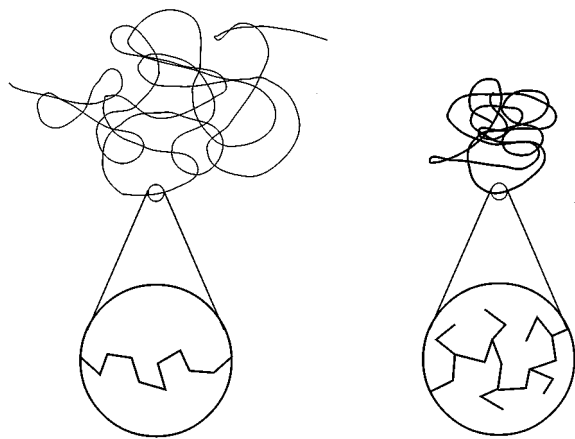


FIG. 1. Illustration of the pure-component parameters $\beta_K = b_K^2 / (6v_m)$ determining conformational asymmetry in the blend: enlargement of the polymer chains shows differing monomer volumes for the same statistical segment length traversed. [The figure is copied from Ref. 14(a), representing the comparison of polyethylene with poly(ethyleneethylene).]

stiffness differs somewhat from the sense of a microscopic rigidity. The latter, for example, may lead to effective intermolecular nematic interactions, which we do not include in our model.) In this paper we let A designate the stiffer species (i.e., we subsequently choose $\epsilon > 1$).

Our treatment of the blend follows our earlier paper on the one-component homopolymer melt,¹¹ to which the reader is directed for a discussion of the self-consistent field approach in greater detail. For the molten blend, we model the Hamiltonian for the polymers as the sum of a Gaussian chain part (for each chain)

$$H_{0,K}[\mathbf{R}_i(s)] = \frac{3}{2b_K^2} \int_0^{N_K} ds \left(\frac{d\mathbf{R}_i}{ds} \right)^2, \quad (2.3)$$

where $\mathbf{R}_i(s)$ parametrizes the configuration of polymer i of species K as a function of the monomer index s , and a coarse-grained excluded-volume interaction part¹⁰

$$H_{\text{int}}[\hat{\rho}(\mathbf{r})] = \frac{1}{2} v \int d\mathbf{r} \hat{\rho}(\mathbf{r})^2 \quad (2.4)$$

which is a functional of the microscopic density

$$\hat{\rho}(\mathbf{r}) = \sum_i \int_0^{N_K} ds \delta(\mathbf{r} - \mathbf{R}_i(s)), \quad (2.5)$$

where the sum runs over polymers of both species. (We have chosen units of energy such that $k_B T = 1$.) The excluded vol-

ume parameter, v , can be considered to be a second Virial coefficient, but can also be related to the bulk monomer density ρ_b and isothermal compressibility κ by the relation

$$v = \frac{1}{\kappa \rho_b^2} \quad (2.6)$$

to lowest order in $1/N_K$.¹¹ This description of the molten blend also applies when there is a small amount of neutral background solvent present, which acts to allow density fluctuations.

To focus on the effect of conformational asymmetry, we have not included any other specific interactions between unlike species; i.e., we have taken the Flory χ parameter (a measure of enthalpic and entropic contributions to the excess free energy of mixing) to be zero. Such a species-specific interaction would have resulted in the excluded volume parameter v being generalized to v_{AA} , v_{AB} , and v_{BB} . Moreover, we treat the surface as infinitely repulsive and neglect any attractive wall-polymer interactions that might give rise to enthalpic contributions to the exchange surface potential.

With this model in mind, we describe such a blend in contact with a surface (either solid, air, or vacuum) in terms of a self-consistent mean-field theory, which can be derived from a saddle-point evaluation of the partition function implied by the Hamiltonian given above.^{7,10,12} In this approach, the interaction H_{int} of a polymer with other polymers is replaced by the interaction of a polymer with a mean-field potential

$$U(\mathbf{r}) = v \rho_b [\tilde{\rho}(\mathbf{r}) - 1], \quad (2.7)$$

where $\tilde{\rho}(\mathbf{r}) = \rho(\mathbf{r})/\rho_b$ is the total monomer density normalized by its bulk value, ρ_b . [The total monomer density $\rho(\mathbf{r})$ is the sum of the two monomer densities $\rho_K(\mathbf{r})$ of species K]. The zero of potential energy (which does not affect the resulting density profiles) has been chosen so that $U(\mathbf{r})$ is zero in the bulk and so describes a harmonic free energy penalty for fluctuations about the bulk density. This form for the potential is identical to that used by Helfand *et al.*^{7,12} It involves the additional assumptions of random mixing, and composition-independent densities and compressibilities. Further discussion of this approximation can be found in Refs. 7, 10, and 12. Finally, we note that the self-consistent potential $U(\mathbf{r})$ felt by either species of polymer is the same, resulting from the fact that the original interaction Hamiltonian is symmetric under interchange of the two species.

The statistics of a polymer of species K in a potential $U(\mathbf{r})$ can be described by the Green's function for observing monomer s at point \mathbf{r} and monomer s' at point \mathbf{r}' , as given by

$$G_K(\mathbf{r}, \mathbf{r}'; s, s') = \frac{\int \mathcal{D}\mathbf{R}(s^*) e^{-\{H_{0,K}[\mathbf{R}(s^*)] + \int ds^* U(\mathbf{R}(s^*))\}} \delta(\mathbf{R}(s) - \mathbf{r}) \delta(\mathbf{R}(s') - \mathbf{r}')}{\int \mathcal{D}\mathbf{R}(s^*) e^{-H_{0,K}[\mathbf{R}(s^*)]} \delta(\mathbf{R}(s) - \mathbf{r})}, \quad (2.8)$$

where the path integral is performed over paths $\mathbf{R}(s^*)$ with $s^* \in [s, s']$. Following Helfand,^{7,12} we simplify our analysis in the presence of a surface by considering the reduced partition function for a chain of length s with an end at position z (the normal component of \mathbf{r} as measured from the wall)

$$Q_K(z, s) = \int d\mathbf{r}' G_K(\mathbf{r}, \mathbf{r}'; s, 0) \quad (2.9)$$

which satisfies the differential equation

$$\left[\partial_s - \frac{b_K^2}{6} \partial_z^2 + U(z) \right] Q_K(z, s) = 0 \quad (2.10)$$

with boundary conditions

$$Q_K(z, 0) = 1; \quad Q_K(0, s) = 0; \quad \text{and} \quad Q_K(\infty, s) = 1. \quad (2.11)$$

The first of these follows directly from the definition of $G(\mathbf{r}, \mathbf{r}'; s, s')$ and the third reflects the fact that the chain is field-free at large distances from the wall. ($U=0$ in the bulk.) The second condition is the appropriate boundary condition for an impenetrable wall in the limit of large number of monomers. We note that we neglect packing effects here (which lead for example to oscillations in the density near the surface) and employ the simple compressibility model as a means to explore the effects of the conformational parameter β .

The monomer density for species K can then be written as

$$\rho_K(z) = \frac{f_K \rho_b}{N_K} \int_0^{N_K} ds Q_K(z, s) Q_K(z, N_K - s), \quad (2.12)$$

where f_K is the bulk mole fraction of K monomers. (Note we have considered the pure components and the blend to have the same total monomer volume fraction, and so $f_A + f_B = 1$.)

Equation (2.12) for the monomer densities in terms of the potential, and Eq. (2.7) for the potential in terms of the monomer density are at this point to be solved self-consistently. However, let us first consider what characteristics of the solution to expect. For the case where the two components are identical, i.e., for a homopolymer melt, the monomer density is characterized by a short-ranged depletion at the wall having thickness

$$\xi_K \equiv \frac{\beta_K}{\rho_b} \sqrt{\frac{2}{v}} = \frac{b_K}{\sqrt{3v\rho_b}} \quad (2.13)$$

(which is simply the Edwards bulk correlation or screening length) followed by a small $\mathcal{O}(N^{-3/2})$ excess on the R_g scale. For a melt, ξ is typically on the order of a monomer size. The “inner” depletion solution, which to lowest order is independent of N , thus matches onto an “outer” solution with a range that grows as \sqrt{N} . In the outer regime, the potential can be neglected in comparison with the other terms in Eq. (2.10), leaving the free-polymer equation

$$\left[\partial_s - \frac{b_K^2}{6} \partial_z^2 \right] Q_K(z, s) = 0. \quad (2.14)$$

The inner solution can thus be considered to produce effective boundary conditions for the outer solution of $Q_K(z, s)$ in

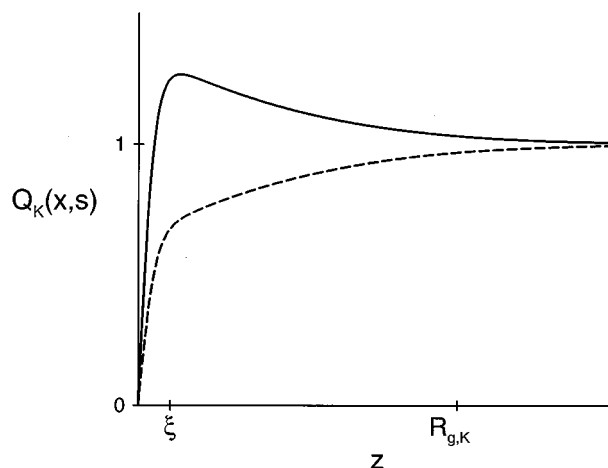


FIG. 2. Depiction of the inner and outer solutions for the functions $Q_K(z, s)$: the inner solution is determined by the ratio of β_K with the bulk screening length ξ . This then matches to an outer solution on the $R_{g,K}$ scale in a field-free region of space. The solid line is for component B (lower β), and the dashed line for component A (higher β).

Eq. (2.14). Due to the free energy penalty for fluctuations of the density from its bulk value, this outer solution is constrained to be relatively flat. However, since no such constraint holds for fluctuations of *composition* in the case of blends, we can expect a short ranged depletion to join onto an $\mathcal{O}(1)$ enrichment having a range on the order of R_g from the surface, as is sketched in Fig. 2.

A nearly incompressible, single-component homopolymer melt must experience a strong localized potential near a surface in order to produce larger-scale reflecting boundary condition statistics on the chains, and hence a flat density profile.¹¹ This nearly flat profile creates an attractive potential well in the surface depletion region that precisely screens the effective entropic repulsion from a sharp surface—in effect, as first articulated by de Gennes,¹³ a sum rule exists for the self-consistent potential. The strength of the potential required to screen the surface, however, depends on β . In the present case of a conformationally asymmetric blend, where polymers with different β feel the *same* potential, we necessarily find ourselves in the situation where the surface repulsion is underscreened for one component (the stiffer species), and overscreened for the other. The degree of over or underscreening is determined by the matching of inner and outer solutions self-consistently, which we present in the next section.

III. WEAK SURFACE SEGREGATION

We proceed by first examining the case of weak segregation of one component at the surface. Since small differences in β can lead to bulk phase separation,¹⁴ we anticipate that the composition profiles depend very sensitively on the conformational asymmetry, and so analyze our equations within perturbation theory in $(\epsilon-1)$ about a reference where the two components are identical, each having a mean value of β given by

$$\beta^2 \equiv \frac{1}{2}(\beta_A^2 + \beta_B^2). \quad (3.1)$$

(Unsubscripted quantities in this section denote the corresponding value in the reference system.) It will be shown that the perturbation expansion is valid up to the same critical value of $(\epsilon-1)$ at which the components are predicted to phase separate in the bulk. We express the full reduced partition function and density in terms of perturbed quantities (denoted by overbars) as

$$\begin{aligned} Q_K(z, s) &= Q_0(z, s) + (\epsilon-1)\bar{Q}_K(z, s), \\ \bar{\rho}(z) &= \bar{\rho}_0(z) + (\epsilon-1)\bar{\rho}(z), \end{aligned} \quad (3.2)$$

where $Q_0(z, s)$ and $\bar{\rho}_0(z)$ are the unperturbed reference functions (where $b_A = b_B = b$), and $(\epsilon-1)\bar{Q}_K(z, s)$ and $(\epsilon-1)\bar{\rho}(z)$ are the first-order corrections. From Eq. (2.12), $\bar{\rho}(z)$ is given in terms of the $\bar{Q}_K(z, s)$ to lowest order in $(\epsilon-1)$ by

$$\bar{\rho}(z) = \frac{2}{N} \int_0^N ds \, Q_0(z, s) \bar{Q}_+(z, N-s), \quad (3.3)$$

where

$$\bar{Q}_+(z, s) = f_A \bar{Q}_A(z, s) + f_B \bar{Q}_B(z, s). \quad (3.4)$$

We have also chosen to examine the simplest case of equal N (molecular volumes) for both components, and discuss the case of $N_A \neq N_B$ in Sec. V.

The equations for \bar{Q}_K to first order in $(\epsilon-1)$ then reduce to

$$\begin{aligned} \left[\partial_s - \frac{b^2}{6} \partial_z^2 + v \rho_b (\bar{\rho}_0(z) - 1) \right] \bar{Q}_K(z, s) \\ = \left(\theta_K \frac{b^2}{12} \partial_z^2 - v \rho_b \bar{\rho}(z) \right) Q_0(z, s), \end{aligned} \quad (3.5)$$

where θ_K is an Ising-like variable defined by $\theta_A = +1$, $\theta_B = -1$. In other words, within perturbation theory, the difference functions \bar{Q}_K , which control changes in the composition profiles, satisfy the same differential equation as Q_K , but with inhomogeneous source terms involving \bar{Q}_+ [via the term $\bar{\rho}(z)$]. In turn, \bar{Q}_+ , which controls changes in the total density profile, satisfies a related inhomogeneous linear equation

$$\begin{aligned} \left[\partial_s - \frac{b^2}{6} \partial_z^2 + v \rho_b (\bar{\rho}_0(z) - 1) \right] \bar{Q}_+(z, s) + v \rho_b \bar{\rho}(z) Q_0(z, s) \\ = (f_A - f_B) \frac{b^2}{12} \partial_z^2 Q_0(z, s). \end{aligned} \quad (3.6)$$

A. Ground state analysis

We first attempt to solve the equations within ground state ($N \rightarrow \infty$, $\partial_s \rightarrow 0$). While this approach generates perturbations to the composition profiles that diverge with the system size, it elucidates the nature of the effective boundary conditions, and can be used as a starting point for calculating profiles for finite molecular weight.

With the unperturbed ground state reference functions¹¹ given by $Q_0(z) = \tanh(z/\xi)$ and $\bar{\rho}_0(z) = \tanh^2(z/\xi)$, the perturbation in the density satisfies

$$\bar{\rho}(z) Q_0(z) = 2 \bar{\rho}_0(z) \frac{1}{N} \int_0^N ds \, \bar{Q}_+(z, s) \quad (3.7a)$$

$$= 2 \bar{\rho}_0(z) \bar{Q}_+(z), \quad (3.7b)$$

where in our analysis of ground state, we drop the dependence on s , to be replaced by the limiting $s \rightarrow \infty$ value. Neglecting the terms involving ∂_s in Eqs. (3.5) and (3.6) results in the ground state equations

$$-\frac{b^2}{6} \partial_z^2 \bar{Q}_K + v \rho_b (\bar{\rho}_0 - 1) \bar{Q}_K = \theta_K \frac{b^2}{12} \partial_z^2 Q_0 - 2 \rho_b \bar{\rho}_0 \bar{Q}_+, \quad (3.8)$$

where \bar{Q}_+ is given by solving

$$-\frac{b^2}{6} \partial_z^2 \bar{Q}_+ + v \rho_b (3 \bar{\rho}_0 - 1) \bar{Q}_+ = (f_A - f_B) \frac{b^2}{12} \partial_z^2 Q_0. \quad (3.9)$$

These ground state equations can only be solved in a finite box, with boundary conditions specified at the walls. (The ∂_s terms are necessary to satisfy the boundary conditions at $z = \infty$ in a semi-infinite system.) As required by Eq. (2.11), the finite slab boundary conditions are

$$\begin{aligned} \bar{Q}_+(z=0) &= \bar{Q}_+(z=L) = 0, \\ \bar{Q}_K(z=0) &= \bar{Q}_K(z=L) = 0. \end{aligned} \quad (3.10)$$

Equations (3.8) and (3.9) can then be solved exactly to yield

$$\bar{Q}_{+,GS}(z) = -\frac{1}{4} (f_A - f_B) \frac{z}{\xi} \operatorname{sech}^2(z/\xi), \quad (3.11a)$$

$$\begin{aligned} \bar{Q}_{K,GS}(z) &= \bar{Q}_{+,GS}(z) + \theta_K \frac{2}{3} (1 - f_K) \\ &\quad \times \{ \ln[\cosh(z/\xi)] - c_L \} \tanh(z/\xi). \end{aligned} \quad (3.11b)$$

The number c_L in Eq. (3.11b) is the unique multiplier of the homogeneous solution $\tanh(z/\xi)$ chosen to satisfy the $z=L$ boundary conditions, and has the large L asymptotic behavior

$$c_L \sim L/\xi - \ln(2). \quad (3.12)$$

The expression for the linear correction $\bar{Q}_{+,GS}(z)$ corresponds to a shift in the correlation length ξ from its reference value to a composition-weighted average. In particular, the expression given by Eq. (3.11a) corresponds to the first order change when the density is given by the superposition

$$\bar{\rho}(z) = f_A \tanh^2(z/\xi_A) + f_B \tanh^2(z/\xi_B). \quad (3.13)$$

As the surface tension for the blend with the model Hamiltonian considered here can be written as a functional of only the total monomer density,¹¹ the superposition principle above applies also to the surface tension γ

$$\gamma = f_A \gamma_A + f_B \gamma_B, \quad (3.14)$$

where $\gamma_K = (2/3) \xi_K v \rho_b^2$ are the pure-component surface tensions. While Eq. (3.14) is only strictly valid in the perturbative limit, a possible useful generalization which holds in the opposite limit of strong segregation is to replace the f_K by

their values at the surface. As for the composition profile, the form of the solution for $\bar{Q}_{K,GS}$ is a rise from zero at the wall to a height $-\theta_K(2/3)(1-f_K)L/\xi$ within a distance ξ , followed by a linear decline for the rest of the box length L with slope $\theta_K(2/3)(1-f_K)/\xi$.

The ground state analysis of these equations illustrates the sensitivity of the surface composition to the parameter ϵ . Because the ground state solution, which corresponds to infinitely long chains, depends on the size of the system, L , the amplitude of the segregation is never small, no matter how small the conformational asymmetry ($\epsilon-1$). That the amplitude of the composition profile is seen to grow with the size of the box is a signature of the preferred component completely expelling the other component away from the surface to the other end of the box. The associated linear profile can be considered to arise within ground state in order to satisfy effective constant flux boundary conditions at the wall. In contrast, when we consider *finite chains* that are smaller than the box size, we shall see that the profiles decay on the scale of R_g , while satisfying the same effective slope conditions at the wall.

B. Finite chain length

To account for finite chain length, we reintroduce the term ∂_s into Eq. (3.8). While the composition profile in ground state, \bar{Q}_K , can be of macroscopic extent, the total density still relaxes to its bulk value within a microscopic length (as is evident from the correction \bar{Q}_+). In particular, the density profile required in Eq. (3.8) is that of a homopolymer melt of chains of finite length N , which can be shown to differ from the ground state profile $\bar{\rho}_0(z)$ by a shift of order $1/N$ in the surface region.^{11,15} Since this shift is in general small compared to those in Eq. (3.13) due to conformational asymmetry, we can approximate the density $\rho(z)$, its shift $\bar{\rho}(z)$, and Q_0 by their ground state values.

Since the zeroth-order reference solutions already satisfy the existing boundary conditions, the appropriate boundary conditions on the perturbation terms \bar{Q}_K are simply

$$\bar{Q}_K(z,0)=0; \quad \bar{Q}_K(0,s)=0; \quad \text{and} \quad \bar{Q}_K(\infty,s)=0 \quad (3.15)$$

leading to the solution

$$\bar{Q}_K(z,s)=\bar{Q}_{K,GS}(z)-\int_0^\infty dz' G_0(z,z';s)\bar{Q}_{K,GS}(z'), \quad (3.16)$$

where $G_0(z,z';s)$ is the Green's function for the reference (homopolymer) melt in ground state. In particular, G_0 satisfies the equation

$$\left[\partial_s - \frac{b^2}{6} \partial_z^2 + v \rho_b(\bar{\rho}_0(z)-1) \right] G_0(z,z';s) = \delta(z-z') \delta(s). \quad (3.17)$$

The full solution represented by Eq. (3.16) (described in further detail in the Appendix) exhibits a matching of an inner depletion region to an outer solution on the R_g scale. However, a useful approximate solution in the regime of physical interest $\xi \ll z \ll R_g$ (recall that ξ is a monomer size scale in a melt) is given to lowest order in $(\epsilon-1)$ by

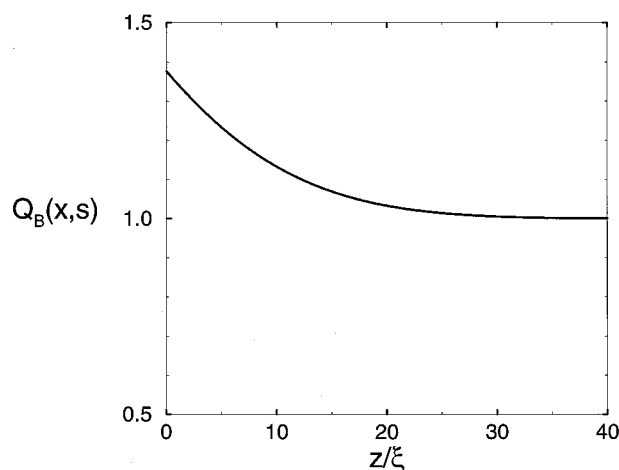


FIG. 3. Coarse-grained outer solution for $Q_B(z,s)$ in Eq. (3.18). The figure was plotted for parameter values $b=\xi$, $R_g=10\xi$, $f_B=1/2$, and with a conformational asymmetry of $\epsilon-1=.1$.

$$Q_K(z,s) \approx 1 - \theta_K(\epsilon-1) \frac{2\sqrt{6}}{9} (1-f_K) \frac{\sqrt{s}b}{\xi} \times \left[\frac{1}{\sqrt{\pi}} \exp(-Z_s^2) - Z_s \operatorname{erfc}(Z_s) \right], \quad (3.18)$$

where $Z_s = z/(2\sqrt{s}b^2/6)$ and $\operatorname{erfc}(z)$ is the complementary error function. This coarse-grained profile is shown in Fig. 3. (For $Z_s > 1$, there is a rapid exponential decay to unity.) Since the potential is nearly flat in the outer region of $z > \xi$, this solution can also be obtained by solving the free polymer differential equation Eq. (2.14), but with effective boundary conditions that will be specified in detail below.

From Eq. (3.7a), the density of species K is given in the outer region ($z > \xi$) by

$$\bar{\rho}_K(z) \approx f_K - \theta_K(\epsilon-1) \frac{16}{9} f_A f_B \frac{R_g}{\xi} F_\rho(z/2R_g), \quad (3.19)$$

where the shape of the profile is given by the function

$$F_\rho(Z) = \left[\frac{1}{\sqrt{\pi}} (1+Z^2) e^{-Z^2} - \left(\frac{3Z}{2} + Z^3 \right) \operatorname{erfc}(Z) \right]. \quad (3.20)$$

The more flexible species thus segregates to the surface, expelling the less flexible species. The magnitude of the segregation is proportional to the conformational asymmetry, the square root of the molecular weight, the product of the volume fractions, and increases as the blend becomes less compressible ($\xi \rightarrow 0$). The *amplitude* of the surface enrichment, i.e., the ratio of surface compositions just beyond the inner region, is given by

$$\frac{\bar{\rho}_A(z=0^+)}{\bar{\rho}_B(z=0^+)} = \frac{f_A}{f_B} \left(1 - \frac{16}{9\sqrt{\pi}} \frac{(\epsilon-1)R_g}{\xi} \right). \quad (3.21)$$

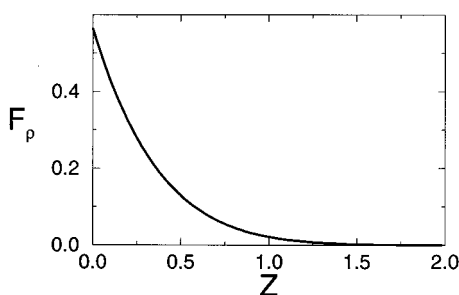


FIG. 4. The shape function $F_p(Z)$ in Eq. (3.20) entering in the composition profile $\tilde{\rho}(z)$.

The range of the surface enrichment is on the order of the radius of gyration, R_g , of the chains; the composition profile decays rapidly beyond R_g . The form of the composition profile $F_p(Z)$ is displayed in Fig. 4.

The above perturbative results are valid when the perturbation $(\epsilon-1)\bar{Q}_K$ is small compared to the unperturbed value $f_{K0}Q_0$. It is easily verified that this condition is satisfied for

$$(\epsilon-1) \ll \frac{\xi}{b\sqrt{N}}. \quad (3.22)$$

Since for a molten blend, ξ is on the order of a monomer size b , the above criteria is satisfied for the range of validity desired, i.e., conformational asymmetry sufficiently weak that bulk phase separation is avoided.¹⁴

IV. EFFECTIVE SURFACE POTENTIAL AND BOUNDARY CONDITIONS

Since the ground state energy of the potential can be considered as an adsorption free energy per monomer, the above analysis suggests that segregation profiles might be deduced from a surface potential that favors one of the two components. Indeed, in this section we demonstrate that the coarse-grained profiles for $Q_K(z)$ in Eq. (3.18) are identical to that for a polymer in the presence of an appropriately selected delta function surface potential. This delta function potential can be considered to be located infinitesimally close to the wall at which the polymer, in the absence of the potential, would obey reflecting boundary conditions (as is appropriate for a homopolymer melt). For convenience, we can use the fact that polymer statistics in reflecting boundary conditions are equivalently generated in a free infinite space (i.e., having positive and negative values of z) with all sources and potentials reflected about $z=0$ additively. In particular, for the case under consideration, the sum of the delta function and its reflected image simply corresponds to a delta function situated at the origin with double the original strength. We therefore consider a potential of the form

$$U_K(z) = 2U_K\delta(z), \quad (4.1)$$

where U_K represents the effective surface field in the problem, and will be determined by establishing the value which reproduces the profiles found in Sec. III. (Note that the surface exchange potential μ_1 discussed in the Introduction is

related to the U_K by $\mu_1 = U_A - U_B$.) Using Eq. (4.1) in Eq. (2.10) extended to negative z then yields the differential equation

$$\left[\partial_s - \frac{b_K^2}{6} \partial_z^2 + 2U_K\delta(z) \right] Q_K(z,s) = 0 \quad (4.2)$$

with boundary conditions

$$Q_K(z,0) = 1 \quad \text{and} \quad Q_K(\pm\infty, s) = 1. \quad (4.3)$$

Similarly, the differential equation for the corresponding Green's function is

$$\left[\partial_s - \frac{b_K^2}{6} \partial_z^2 + 2U_K\delta(z) \right] G_K(z,z';s,0) = \delta(z-z')\delta(s) \quad (4.4)$$

which can be solved by a Laplace transform in the variable s , evaluating the inverse of the differential operator, and inverting the Laplace transform. The solution is

$$G_K(z,z';s,0) = \frac{\sqrt{3}}{b_K\sqrt{2\pi s}} e^{-3(z-z')^2/2sb_K^2} - \frac{3U_K}{b_K^2} \times e^{6U_K(|z|+|z'|+U_Ks)/b_K^2} \times \text{erfc}\left(\frac{\sqrt{3}(|z|+|z'|+2U_Ks)}{b\sqrt{2s}}\right). \quad (4.5)$$

The Green's function for the physical problem at a surface of a semi-infinite space with $z, z' > 0$ is then the reflected sum

$$G_K(z,z';s,0) = G_{K,\text{refl}}(z,z';s,0) - \frac{6U_K}{b_K^2} \times e^{6U_K(z+z'+U_Ks)/b_K^2} \times \text{erfc}\left(\frac{\sqrt{3}(z+z'+2U_Ks)}{b\sqrt{2s}}\right), \quad (4.6)$$

where

$$G_{K,\text{refl}}(z,z';s,0) = \frac{\sqrt{3}}{b_K\sqrt{2\pi s}} [e^{-3(z-z')^2/2sb_K^2} + e^{-3(z+z')^2/2sb_K^2}] \quad (4.7)$$

is the *free* Green's function for reflecting boundary conditions.

With the full Green's function in hand, we can calculate the quantities of interest for the problem of a polymer blend at a surface. The solution for the profiles $Q_K(z,s)$ follow directly from Eq. (2.9) as

$$Q_K(z,s) = \Phi\left(\frac{\sqrt{3}z}{b_K\sqrt{2s}}\right) + e^{6(U_Kz+U_K^2s)/b_K^2} \times \text{erfc}\left(\frac{\sqrt{3}(z+2U_Ks)}{b_K\sqrt{2s}}\right), \quad (4.8)$$

where $\Phi(z) = 1 - \text{erfc}(z)$ is the error function.

Several physical limits are immediately accessible. For $U_K/b_K \ll 1/\sqrt{s}$, we obtain the perturbative result

$$Q_K(z, s) \approx 1 - \frac{2\sqrt{3}U_K}{b_K} \left[\sqrt{\frac{2s}{\pi}} e^{-3z^2/2sb_K^2} - \frac{\sqrt{3}z}{b_K} \operatorname{erfc}\left(\frac{\sqrt{3}z}{b_K\sqrt{2s}}\right) \right] \quad (4.9)$$

in agreement with Eq. (3.18) when the strength of the potential per monomer is assigned the value

$$\begin{aligned} \frac{U_K}{b_K} &= \theta_K \frac{1}{9} (\epsilon - 1)(1 - f_K) \frac{b_K}{\xi} \\ &\approx \theta_K \frac{2}{9} (1 - f_K) \frac{b_A - b_B}{\xi}. \end{aligned} \quad (4.10)$$

Additionally, for the case of precise screening of the wall in a homopolymer melt, i.e., $U_K = 0$, we find $Q_K(z, s) = 1$, as appropriate for reflecting boundary conditions.

For large positive U_K we note that

$$\begin{aligned} G_K(z, z'; s, 0) &\approx \frac{\sqrt{3}}{b_K\sqrt{2\pi s}} \left[e^{-3(z-z')^2/2sb_K^2} - e^{-3(z+z')^2/2sb_K^2} \right], \\ Q_K(z, s) &\approx \Phi\left(\frac{\sqrt{3}z}{b_K\sqrt{2s}}\right) \end{aligned} \quad (4.11)$$

which corresponds to the *absorbing boundary condition* Green's function for a polymer near a hard wall. For moderately large negative U_K , we find

$$\begin{aligned} G_K(z, z'; s, 0) &\approx \frac{-12U_K}{b_K^2} e^{-E_{GS}s} Q_{GS}(z) Q_{GS}(z'), \\ Q_K(z, s) &\approx 2e^{-E_{GS}s} Q_{GS}(z), \end{aligned} \quad (4.12)$$

where

$$\begin{aligned} Q_{GS}(z) &= e^{6U_K|z|/b_K^2}, \\ E_{GS} &= -\frac{6U_K^2}{b_K^2} \end{aligned} \quad (4.13)$$

are the (bound) ground state solution and energy corresponding to the adsorption of polymer to the surface. For the blend, the more flexible polymer is adsorbed and the stiffer repelled from the wall; however, as discussed below, corrections (derivable from a linear response theory) must be added to achieve self-consistency in the composition profiles for strong segregation.

It is possible to describe the above perturbative solutions within linear response theory, given that the wall produces a local surface potential. We mainly remark that the expressions for $Q_K(z, s)$ and for $\bar{\rho}_K(z)$ implied by Eqs. (3.18) and (3.19) can also be written in the form

$$\begin{aligned} \bar{Q}_K(z, s) &= -\frac{s}{2\rho_b} \int_{-\infty}^{\infty} dz' S_{eU}^K(z, z'; s) U_K(z'), \\ \bar{\rho}_K(z) &= -\frac{f_K}{\rho_b} \int_{-\infty}^{\infty} dz' S_{\rho U}^K(z, z') U_K(z') \end{aligned} \quad (4.14)$$

with the same surface potential $U_K(z')$ given by Eq. (4.1) and with strength U_K given identically by Eq. (4.10). The response functions for field-free chains appearing in the above are

$$S_{eU}^K(z, z'; s) = \frac{2\rho_b}{\sqrt{s}b_K^2/6} \left[\frac{1}{\sqrt{\pi}} \exp(-Z_s^2) - Z_s \operatorname{erfc}(Z_s) \right] \quad (4.15)$$

for the response of the density of ends of polymers of length s to a potential acting on all s monomers, and

$$S_{\rho U}^K(z, z') = N_K \rho_b \frac{4}{3R_{g,K}} F_{\rho}(z/2R_{g,K}) \quad (4.16)$$

for the response of the total monomer density of a polymer of length N_K to a potential acting on all N_K monomers. We note that $(4/3R_{g,K})F_{\rho}(z/2R_{g,K})$ is merely the real space representation of the one-dimensional Fourier transform of the Debye function.

A. Effective boundary conditions

The preceding analysis clearly demonstrates that the more flexible polymer experiences an effective surface adsorption potential, while the stiffer polymer feels a repulsion at the wall. For either polymer, the statistics for weak segregation (as described by the Green's function) are consistent with a localized surface potential augmented by reflecting boundary conditions. The delta function potential leads to a cusp at the origin in the normalized eigenfunctions associated with Eq. (4.2), with a discontinuity in the slope that is proportional to the strength of the potential. Given the reflection symmetry imposed by the boundary conditions, it can be shown that the eigenfunctions, and hence the Green's function in Eq. (4.6) and the $Q_K(z, s)$ functions in Eq. (4.8), are free-space solutions that obey effective mixed boundary conditions of the type

$$\partial_z G_K(z, z'; s, s')|_{z=0} = \frac{6U_K}{b_K^2} G_K(z, z'; s, s')|_{z=0} \quad (4.17a)$$

and

$$\partial_z Q_K(z, s)|_{z=0} = \frac{6U_K}{b_K^2} Q_K(z, s)|_{z=0}. \quad (4.17b)$$

In the perturbative regime, $Q_K(z, s)|_{z=0} \approx 1$, and so the effective boundary condition can also be considered to be that of constant flux

$$\partial_z Q_K(z, s)|_{z=0} = \frac{6U_K}{b_K^2} = \theta_K \left(\frac{2}{3} \right) \frac{(\epsilon - 1)(1 - f_K)}{\xi}. \quad (4.18)$$

Thus reflecting boundary conditions for a given component are approached as the blend is made more conformationally symmetric or compressible, or more pure in that component.

Moreover, since the fluxes are equal and opposite (after weighting by f_K), the constraint of uniform density is automatically satisfied by these boundary conditions.

In summary, the mixed boundary condition can be understood for the $Q_K(z,s)$ functions as follows. For the case of a one-component homopolymer melt, the ground state of the potential has zero eigenvalue, resulting in a flat profile (zero slope) and effective reflecting boundary conditions. In the case of a blend, the two species segregate near the surface according to their β parameters, with the potential experienced by the stiffer (more flexible) species having a small positive (negative) eigenvalue, resulting in a profile with logarithmic slope that is proportional to the effective surface field. This form for the mixed boundary conditions in the perturbative limit is equivalent to constant slope boundary conditions.

V. DISCUSSION AND CONCLUSIONS

We have examined the effect of conformational asymmetry on surface segregation in an otherwise symmetrical polymer blend. Our calculations have demonstrated that for flexible chains, significant segregation of the smallest β component to a surface can occur for purely *entropic* reasons. The magnitude of the enrichment of the small β species is proportional to the product of the conformational asymmetry parameter, $(\epsilon-1)$, the radius of gyration of the chains, $R_{g,K}$ and the inverse of the bulk screening length, ξ . Moreover, we have shown that this enrichment is consistent with an effective surface exchange potential μ_1 of strength that scales according to the simple arguments leading to Eq. (1.2), i.e., $\mu_1 \sim (\epsilon-1)/\xi$.¹⁶ While we have presented a detailed description of the composition profile and configurational statistics of such a blend at a surface, the enrichment by the more flexible species can be simply understood as follows. The enriched species is the one that is less perturbed free-energetically by the surface, i.e., has the lower surface tension. As the more flexible species has a shorter bulk correlation length, it can heal to the bulk density within a shorter distance from the wall, and thereby incur a smaller square-gradient (conformational entropy) and interaction (excluded-volume entropy) cost relative to the stiffer species. Finally, we have shown that the perturbative regime of weak segregation analyzed in the present paper corresponds to the one-phase regime for a *bulk* mixture of conformationally asymmetric polymers.¹⁴

Our analysis was restricted to the case of equal chain lengths, i.e., equal values of N_K . While corrections to the density profile in one-component melts arising from length differences scale as $N^{-3/2}$ and are subdominant to the effects we consider here, because of the surface field due to conformational asymmetry, the amplitude of the surface composition enrichment in a blend scales as \sqrt{N} . For differing values of N , this leads to a total density that is not "consistent" with the flat ground state density profile. To rectify this, a pressure field is generated that has a length scale intermedi-

ate between those of the two polymer R_g 's. This self-consistent pressure field can in principle be accounted for with a type of RPA calculation, much as in our previous treatments of single-component melts near a wall,¹¹ and of blends of branched and linear polymers near a wall.¹⁷

Donley¹⁸ has recently carried out numerical evaluations of essentially the same self-consistent field equations employed here for modeling surface enrichment in binary polymer blends. In addition, he has explored the case of additional *bulk* interactions between the two species described by an enthalpic Flory χ parameter. Donley's calculations were done with a large but finite harmonic compressibility field corresponding to Eq. (2.7). The numerical results presented there are in agreement with our perturbative analytic predictions for the dependences on molecular weight and compressibility, and also with the effective boundary conditions on the outer solution. More strikingly, Donley has also varied R_g and V_{mol} independently, and has determined the relation between the two such that there is no effective surface segregation relative to the bulk. His results corroborate our finding that $(\epsilon-1)$ is the parameter that controls the sign of surface enrichment, and should be minimized in order to suppress surface segregation in blends with no enthalpic contributions to the surface potential. These findings differ from those of an earlier density functional theory,⁴ which incorrectly identified a different combination of R_g and V_{mol} as the controlling parameter. The density functional theory, while predicting the same sign of segregation, relied on a gradient expansion of the effective surface potential, which we have shown here to be singular.

As pointed out in Sec. I, surface segregation in binary polyolefin blends and copolymers is very likely controlled by a combination of entropic and enthalpic factors. Neglecting packing effects, we have been able to arrive at a modified β principle for the sign of enrichment in such systems at low energy surfaces. Namely, we predict that the component with the smallest product of β_K and the solubility parameter δ_K will be present in excess at the surface. Since δ_K increases linearly with β_K for a reasonably broad class of polyolefins, it appears that both the entropic and enthalpic factors in this product favor enrichment by the smallest β component, hence explaining the original β principle postulated by Bates and co-workers.³ Moreover, the simulation results of Yethiraj⁵ seem to fit consistently within this picture.

Generalization of the present theory to blends with three or more components is straightforward, the main result being that the magnitude in the change of the surface excess and profile is proportional to the difference of the β parameter of that component relative to the species average. A generalization of the perturbative method used here to include bulk χ interactions is also possible. Such corrections enter only at second order, since for a conformationally symmetric blend with small χ and no enthalpic surface potential, neither species will be favoured at the surface. Our preliminary analysis

indicates that the role of χ , aside from altering the bulk response functions, is to add linearly to the effective surface excluded volume parameter, and hence enhance the exchange surface field towards greater segregation.

The segregation of components in a blend at a surface can have important consequences for the surface tension, surface rheology, tack, and adhesion. While in the case of blends, the conformational asymmetry is highly sensitive to the chemical structure of the two types of segments, for block and graft copolymers there exists the enticing possibility of fine tuning surface properties, since the conformational asymmetry can be more delicately adjusted by changing copolymer architecture (e.g., star blocks).

ACKNOWLEDGMENTS

This work was supported by the MRL program of the National Science Foundation under Award No. DMR-9123048. We thank James Donley and David Morse for helpful discussions.

APPENDIX: SOLUTION FOR THE PERTURBATIVE DIFFERENTIAL EQUATIONS WITH THE GROUND STATE POTENTIAL

To first order, solutions to the perturbative differential equation Eq. (3.5) are found by solving inhomogeneous time-dependent differential equations within the zeroth-order reference potential. As discussed in the paper, we can approximate the reference potential by its ground state value. The evaluation of the coarse-grained behavior for $z \gg 1$ for the finite chain (time-dependent) solutions $Q_K(z, s)$ then proceed along similar lines as for the case of homopolymer. (See Appendix B in Ref. 11.) We outline here the method of solution, and present the main perturbative result for both the inner and outer regions (up to distances of R_g).

The Green's function for the homogeneous version of Eq. (3.5) using the ground state potential is

$$G(z, z'; s) = \frac{1}{\sqrt{2\pi s}} [e^{-(z-z')^2/2s} - e^{-(z+z')^2/2s}] - \frac{1}{4} e^{s/2} \text{sech}(z) \text{sech}(z') \Phi_4(z, z'; s) \quad (\text{A1})$$

where $\Phi_4(z, z'; s)$ is the combination of the four error functions

$$\Phi_4(z, z'; s) = \Phi\left(\frac{s-z-z'}{\sqrt{2s}}\right) - \Phi\left(\frac{s-z+z'}{\sqrt{2s}}\right) + \Phi\left(\frac{s+z+z'}{\sqrt{2s}}\right) - \Phi\left(\frac{s+z-z'}{\sqrt{2s}}\right). \quad (\text{A2})$$

(For simplicity, in this Appendix we have taken lengths such

as z to be in units of ξ , and chemical lengths such as s to be in units of $3\xi^2/b^2$.) The correction $\bar{Q}_K(z, s)$ is then given by Eq. (3.16) as an integral of the Green's function with the ground state solution $\bar{Q}_{K,GS}(z)$ in Eq. (3.11b). Integrating by parts and then using an expansion in zz'/s similar to that employed in Ref. 11 to separate the inner and outer scales, we find for $z < \sqrt{s}$

$$\begin{aligned} \bar{Q}_K(z, s) &= \theta_K(1-f_K) \frac{2}{3} \left\{ [\ln(2 \cosh(z)) - 1] \tanh(z) \right. \\ &\quad \left. - \Phi\left(\frac{z}{\sqrt{2s}}\right) \right. \\ &\quad \times [z \tanh(z) - 1] - \sqrt{\frac{2s}{\pi}} e^{-z^2/2s} \tanh(z) \\ &\quad \left. - \frac{2}{\sqrt{2\pi s}} \frac{\pi^2}{24} e^{-z^2/2s} [\tanh(z) + z/s] \right\} - \frac{(f_A - f_B)}{4} \\ &\quad \times \left\{ z \text{sech}^2(z) - \frac{1}{\sqrt{2\pi s}} e^{-z^2/2s} [\tanh(z) + z/s] \right\}. \quad (\text{A3}) \end{aligned}$$

Applying the further condition that $z \gg 1$ leads to Eq. (3.18) for the coarse-grained profile.

¹K. Binder, *Acta Polymer* **46**, 204 (1995).

²U. Steiner, J. Klein, E. Eiser, A. Budkowski, and L. J. Fetters, *Science* **258**, 1126 (1992).

³(a) A. Karim, N. Singh, M. Sikka, and F. S. Bates, *J. Chem. Phys.* **100**, 1260 (1994); (b) M. Sikka, N. Singh, A. Karim, and F. S. Bates *et al.*, *Phys. Rev. Lett.* **70**, 307 (1993).

⁴G. H. Fredrickson and J. P. Donley, *J. Chem. Phys.* **97**, 8941 (1992).

⁵A. Yethiraj, *Phys. Rev. Lett.* **74**, 2018 (1995).

⁶R. Krishnamoorti, W. W. Graessley, N. P. Balsara, and D. J. Lohse, *Macromolecules* **27**, 3073 (1994).

⁷(a) E. Helfand and Y. Tagami, *J. Chem. Phys.* **56**, 3592 (1972); (b) E. Helfand and Y. Tagami, *ibid.* **57**, 1812 (1972).

⁸J. M. Prausnitz, R. N. Lichtenthaler, and E. G. de Azevedo, *Molecular Thermodynamics of Fluid-Phase Equilibria* (Prentice-Hall, Englewood Cliffs, 1986).

⁹A. Yethiraj, S. K. Kumar, A. Hariharan, and K. S. Schweizer, *J. Chem. Phys.* **100**, 4691 (1994); M. A. Carignano and I. Szleifer, *Europhys. Lett.* **30**, 525 (1995).

¹⁰M. Doi and S. F. Edwards, *The Theory of Polymer Dynamics* (Clarendon, Oxford, 1986).

¹¹D. T. Wu, G. H. Fredrickson, J.-P. Carton, A. Ajdari, and L. Leibler, *J. Poly. Sci., Part B-Polymer Physics* **33**, 2373 (1995).

¹²(a) E. Helfand, *J. Chem. Phys.* **62**, 999 (1975); (b) E. Helfand and A. M. Sapse, *ibid.* **62**, 1327 (1975).

¹³P.-G. de Gennes, *C. R. Acad. Sc. Paris* **290**, série B, 509 (1980).

¹⁴(a) F. S. Bates and G. H. Fredrickson, *Macromolecules* **27**, 1065 (1994);

- (b) G. H. Fredrickson, A. J. Liu, and F. S. Bates, *Macromolecules* **27**, 2503 (1994).
- ¹⁵D. T. Wu and G. H. Fredrickson, *Short and Long Chains at Interfaces: Proceedings of the XXXth Rencontres de Moriond, series: Moriond Condensed Matter Physics: Villars sur Ollon, Switzerland, January 21–28, 1995* (Editions Frontières, Gif-sur-Yvette, 1995).
- ¹⁶In fact, the magnitudes of the surface potentials U_K in Eq. (4.10) result in a value for the surface exchange potential μ_1 which is *identically* equal to the difference between the surface tensions of the corresponding pure homopolymer melts. As shown in Ref. 11, the one-component homopolymer surface tension is given by $\gamma=(2/3)\xi v \rho_b^2$, which corresponds to a value $\alpha=v \rho_b^2/2$ for the interaction density discussed in Sec. I.
- ¹⁷D. T. Wu and G. H. Fredrickson, *Macromolecules* (to be published).
- ¹⁸J. Donley and G. H. Fredrickson, *J. Polym. Sci.: Part B: Polym. Phys.* **33**, 1343 (1995).